

## Temporal scaling of interfaces propagating in porous media

Viktor K. Horváth and H. Eugene Stanley

Center for Polymer Studies and Department of Physics, Boston University, Boston, Massachusetts 02215

(Received 5 June 1995)

To better understand the temporal behavior of a roughening meniscus driven by capillary forces during the imbibition of a viscous fluid in porous media, we measure the height-height autocorrelation function  $C(t)$  using a constant driving force. We find  $C(t) \sim t^\beta$ , with  $\beta = 0.56 \pm 0.03$ , and provide experimental evidence for driving force independent temporal scaling behavior of a propagating wetting front in the presence of quenched noise. We interpret the value of  $\beta$  in terms of the possibility that the dynamics may be governed by nonvanishing nonlinearity due to anisotropic depinning.

PACS number(s): 47.55.Mh, 05.40.+j, 05.70.Ln, 68.35.Fx

The growth of rough surfaces and interfaces under far-from-equilibrium conditions is a common phenomenon in nature [1]. Examples include such processes as vapor deposition, crystallization, thin film growth by atomic beams, settling of granular materials, and fluid flow in porous media. The fluctuations of the interface height  $h(x, t)$  can be characterized either by their standard deviation  $\sigma(l, t)$ , or by the height-height correlation function  $C(l, t) \equiv [(\langle [\tilde{h}(l+x, t+\tau) - \tilde{h}(x, \tau)]^2 \rangle_{x, \tau})]^{1/2}$ , where  $\tilde{h}(x, \tau) \equiv h(x, \tau) - \langle h(x, \tau) \rangle_x$ . The common belief is that  $\sigma(l, t)$  and  $C(l, t)$  exhibit the same general statistical properties.

Particularly useful is the Family-Vicsek dynamic scaling hypothesis [2],

$$C(t) = C(0, t) \sim L^\alpha \mathcal{F}(t/L^{\alpha/\beta}), \quad (1)$$

where  $L$  is the system size and  $\mathcal{F}(y) \sim y^\beta$  for  $y \ll 1$ ,  $\mathcal{F}(y) \sim \text{const}$  for  $y \gg 1$ . Extensive numerical simulations of different computer models [1] predict universal values for the exponents  $\beta$  and  $\alpha$ . Theoretical work is based on Langevin-type equations, such as

$$\frac{\partial h(\mathbf{x}, t)}{\partial t} = v_0 + \nu \nabla^2 h + \lambda_{\text{eff}} (\nabla h)^2 + \eta(\mathbf{x}, t). \quad (2)$$

The linear ( $\lambda_{\text{eff}} = 0$ ) and the nonlinear ( $\lambda_{\text{eff}} \neq 0$ ) cases are referred to as the Edwards-Wilkinson (EW) [3] and Kardar-Parisi-Zhang (KPZ) [4] equations. Analytical solution of Eq. (2) in  $d' = 1$  (where  $d'$  is the dimension of  $\mathbf{x}$ ) reveals the *same* spatial exponent ( $\alpha = 1/2$ ), but *different* temporal exponents

$$\beta_{\text{EW}} = 1/4, \quad \beta_{\text{KPZ}} = 1/3. \quad (3a)$$

If we know these exponents, then we can distinguish between linear and nonlinear dynamics based on  $\beta$ . Therefore it is important to make accurate measurements of  $\beta$ .

If the randomness in the dynamics is due to the inhomogeneity of the media where the moving phase is propagating, then the resulting interface exhibits different scaling behavior. This time-independent "quenched" randomness can be described by replacing  $\eta(\mathbf{x}, t)$  by

$\eta(\mathbf{x}, h(t))$  in Eq. (2). We denote the linear and nonlinear equations as QEW and QKPZ, respectively. Numerical solution of the QEW equation [5] produces self-affine interfaces with a roughness exponent  $\alpha$  in the range  $[0.5 - 1.0]$ , which is tunable with the driving force  $v_0$  [6-10, 12-14]. Different computer models also exhibit very scattered results for  $\alpha$  [7]. However, theoretical considerations suggest [8] that  $\beta_{\text{QEW}} = (4 - d')/4$ . Numerical integration of the QKPZ equation close to the pinning transition exhibits temporal scaling with  $\beta = 0.61 \pm 0.06$ , in good agreement with the result of simple dimensional analysis which predicts  $\beta_{\text{QKPZ}} = (4 - d')/(4 + d')$  [9]. Hence for  $d' = 1$ :

$$\beta_{\text{QEW}} = 3/4, \quad \beta_{\text{QKPZ}} = 3/5. \quad (3b)$$

The fact that scaling of surfaces during roughening in the presence of quenched noise exhibits driving force independent temporal scaling also underlines the importance of the investigation of the exponent  $\beta$ , which is the main goal of this paper.

Specifically, we investigate the growing interface during imbibition of viscous liquids in filter paper. The experimental setup (Fig. 1) contains two vertically positioned

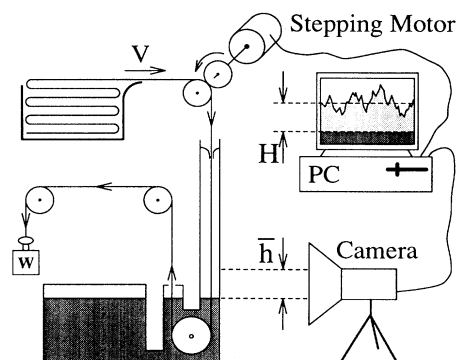


FIG. 1. Schematic of the experimental setup. The average height  $\bar{h}$  of the meniscus in the wetted paper was kept at a constant level. A video camera digitized the interface in real time and the computer pulled down the paper if  $\bar{h}$  became larger than the predefined value  $H$ .

$40 \times 30 \text{ cm}^2$  parallel plexiglass plates separated from each other by 3 cm and closed with side walls. The bottom part of the plates extends into a liquid container from which water starts to wet the filter paper. We designed the size of this liquid container to be large enough to keep the free surface of water at a constant level. All height measurements are relative to this reference level. The upper part of the cell is closed by polyethylene film to prevent a large amount of evaporation. The dry paper passes through two touching cylinders driven by a stepping motor, and enters into the cell through a narrow gap on this film. We use other rollers and a proper weight to keep the paper stretched. Stretching of wet paper sometimes involves changes in the paper structure mostly by elongating the paper strip. This was checked by double measurements of the speed of the paper strip. We measured the speed of the paper both at the driving rollers at the stepping motor, and at the weight used for stretching the paper. Any dilatation of the paper strip would appear in a difference between the speeds at these points. We have used enough small stretching weight to avoid any such difference.

We monitor the wetting front  $h(x, t)$  with a high resolution (0.48 million pixels) CCD NTSC camera horizontally centered in front of the front plate. We use a personal computer to digitize the video image, and to calculate the average height  $\bar{h} = \langle h(x, t) \rangle_x$  in real time. We set our video system to digitize a 8.4-cm-wide segment of the filter paper strip involving a  $110 \mu\text{m}$  (squared) pixel size. We control the motion of the paper by a gear mechanism driven by a stepping motor connected to the same computer. According to our calibration, one step of the motor corresponds to a paper shift of  $\delta y = 85 \mu\text{m}$ .

The water front moves upward in the paper due to the effective driving force  $\varepsilon$ , which is mainly determined by the balance between capillarity and gravity. We maintain this driving force constant by holding  $\bar{h}$  at a predefined value  $H$ . If  $\bar{h}$  exceeds  $H$  by  $\delta y$ , then we pull the paper down by  $\delta y$ . This negative feedback, apart from fluctuations, prescribes a constant average speed  $V$  for the paper for a given  $H$ . Our measurements at 14 different values of  $H$  fit remarkably well the power law

$$V \propto H^{-\Omega}, \quad (4)$$

where  $\Omega = 1.594 \pm 0.007$ , and the quoted uncertainty is the standard deviation from the fitted value. The relation (4) holds in the entire investigated range of the control parameter,  $H \approx [2 \text{ mm}, 40 \text{ mm}]$ , which spans approximately 2.5 decades of the capillary number.

During the experiment, the computer saves the contour lines of the digitized images for later analysis. Snapshots of the evolving interface at different times are superposed in Fig. 2 for three different values of the velocity. We find only a few and negligible [10] overhangs, and when they occur we remove them in the usual way [11].

Using the contour lines we calculated  $C(t)$ , which has less uncertainty than the standard deviation of the interface height, and is therefore more useful for calculating the true exponents [12]. To check the scaling behavior of  $C(t)$ , we form the quantity

$$Y^2(t_i) \equiv \frac{C^2(t_{i+1}) - C^2(t_i)}{t_{i+1}^{2\beta'} - t_i^{2\beta'}} t_i^{2\beta'} \quad (5)$$

where  $t_i, t_{i+1}$  are successive times. If  $C(t) \propto t^\beta$ , then  $Y(t)|_{\beta'=\beta}$  must scale the same way, but provides a more precise (self-consistent) method to determine  $\beta$  by eliminating any existing additive "correction-to-scaling" terms [13]. Figure 3 presents our results for the same data sets as shown in Fig. 2. We find  $Y(t) \propto t^\beta$  for early times and this power-law behavior extends over slightly more than three decades at the minimum driving force ( $V = 1.4 \times 10^{-3} \text{ cm/s}$ ). Within the experimental uncertainty,  $\beta$  is independent of our control parameter  $H$ , yielding an average value

$$\beta_{\text{exp}} = 0.56 \pm 0.03. \quad (6)$$

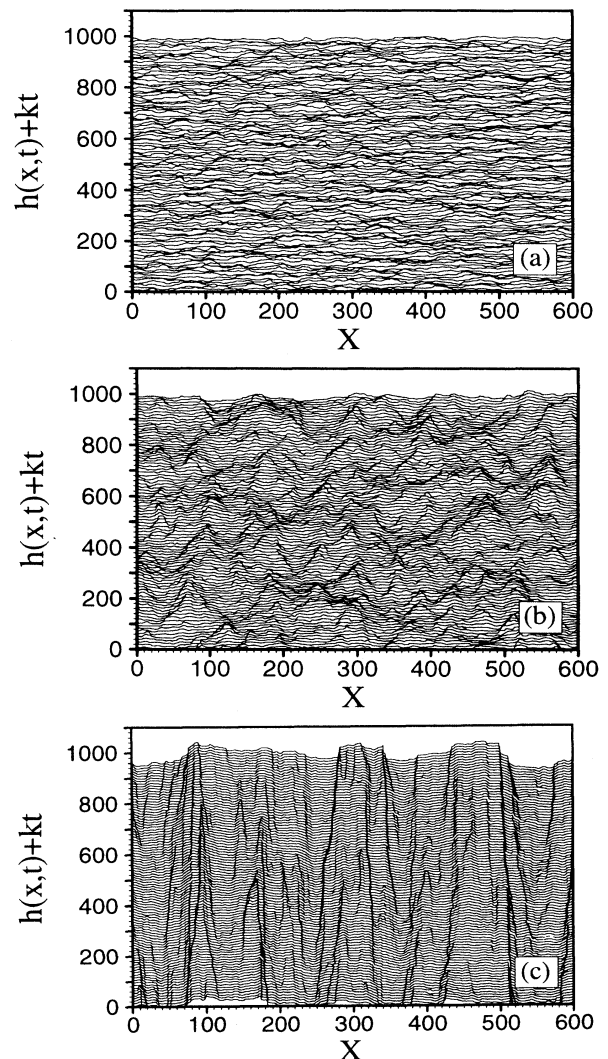


FIG. 2. Snapshots of the evolving interface for different velocities  $V$ . (a)  $V = 4.03 \times 10^{-2} \text{ cm/sec}$ , (b)  $V = 1.32 \times 10^{-2} \text{ cm/sec}$ , (c)  $V = 1.40 \times 10^{-3} \text{ cm/sec}$ . The sampling rate is the same constant for all pictures and the artificial shift  $k$  between the contour lines is proportional to this constant. Units of this figure are in pixels. The pixel/mm ratio is indicated in the text.

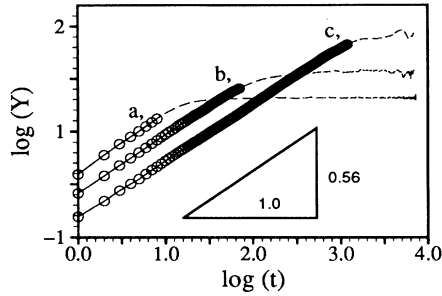


FIG. 3. The differential autocorrelation function  $Y$  vs time is shown by circles. The dashed lines present the saturation regime of the autocorrelation function. The speeds for the three curves are the same as in Fig. 2. Larger speed implies larger intrinsic width (intercept), and smaller saturation value. The base of the logarithm is 10.

This result can be compared to two-dimensional theoretical results and simulations because the small thickness of the filter paper (which is in the order of micrometers) does not permit any coarse-grained roughening perpendicular to the paper strip. Comparing  $\beta_{\text{exp}}$  to (3a), we may exclude the dominance of annealed randomness, which prescribes a much lower value for  $\beta$ . Moreover, the value of  $\beta_{\text{QEW}}$  is also inconsistent with our result. Nevertheless quenched disorder with nonlinear dynamics produces a remarkably close exponent,  $\beta_{\text{QKPZ}} = 0.6$  [9], which suggests that quenched randomness and nonlinearity play important roles in the dynamics of vertical imbibition.

Remarkably, we find no crossover for  $\beta$  in the scaling regime, as might have been expected in the case of QEW [8,14], where the temporal scaling is described by  $\beta_{\text{QEW}}$  for early times and by  $\beta_{\text{EW}}$  for late times (at an intermediate driving force). As the driving force increases, the crossover point  $t^*$  becomes smaller and the scaling region described by  $\beta_{\text{EW}}$  enlarges. From Fig. 3, we observe crossover neither as a function of driving force, nor as a function of time—even at the maximum driving force ( $V = 2.1 \times 10^{-1}$  cm/s). The absence of such a crossover also indicates the importance of the nonlinearity in our experimental system.

It has been observed [15] that numerical results fall into two groups depending on the origin of the nonlinear term  $\lambda(\nabla h)^2$ . Kinematics produces a  $\lambda$  which vanishes at the threshold and the resulting interface belongs to the same universality class where the nonlinear term is absent,  $\lambda_{\text{eff}} = 0$ . On the other side the QKPZ universality class is characterized by a nonvanishing nonlinear term leading to  $(\lambda_{\text{eff}} \neq 0)$ . What is the origin of such a nonlinearity which leads to  $\beta_{\text{exp}} \approx \beta_{\text{QKPZ}}$  in our experiment? Recently Tang, Kardar, and Dhar demonstrated [16] that *anisotropic depinning* yields a nonzero  $\lambda_{\text{eff}}$  at the depinning transition. To illustrate the existence of such an anisotropy in our system, we consider the filter paper as an interconnected network of different capillary tubes. The inhomogeneity of this network can be considered as a random field with amplitude  $\Delta$ . This random field is

correlated isotropically in space within a distance  $a$ , but the driving force (pressure drop) is different along horizontal and vertical tubes,  $F_h = f$  and  $F_v = f - \rho g a$ , respectively, because the driving force must compensate the weight of the liquid in a vertical tube ( $\rho$  is the density of the liquid). Due to this anisotropy, a segment of the interface can easier be pinned vertically than horizontally. Therefore a slope-dependent effective driving force  $\bar{F}(\nabla h) = F(\nabla h) - F_c$  is generated under coarse graining, which explains the absence of large overhangs. Tang *et al.* pointed out [16] that an expansion of  $\bar{F}(\nabla h)$  around its minimum yields to a term  $\lambda_{\text{eff}}(\nabla h)^2$  which remains finite, independent of  $V$ , which is the hallmark of the QKPZ universality class.

Figure 3 demonstrates two effects of increasing the driving force, namely the intercepts increase and the saturated values decrease. In order to incorporate this behavior into the scaling formalism, we assume that Eq. (1) is valid with the rescaled time and space variables  $t'^\beta = t^\beta V^{\theta_t}$  and  $L'^\alpha = L^\alpha V^{-\theta_L}$ . As a consequence of this assumption,  $C(t)_{L,V}$  scales as

$$C(t)_{L,V} \sim V^{-\theta_L} L^\alpha \mathcal{F}\left(t L^{-\alpha/\beta} V^{(\theta_t + \theta_L)/\beta}\right). \quad (7)$$

This extended dynamic scaling (EDS) hypothesis is fully compatible with Eq. (1) for a given  $V$ , but also describes the characteristic role of the driving force in the presence of quenched disorder. In the limit of small driving force and early times ( $t^\beta V^{\theta_t + \theta_L} \ll L^\alpha$ ) the EDS hypothesis reduces to  $C \sim t^\beta V^{\theta_t}$ . For  $t \gg t_c$ , where  $t_c$  is a critical time defined by  $t_c = L^\alpha/\beta V^{-(\theta_t + \theta_L)/\beta}$ , the autocorrelation function is independent of time and saturates at a constant value  $C \sim L^\alpha V^{-\theta_L}$ . This asymptotic behavior is consistent with Fig. 3, as it is expected. In order to perform a quantitative check of Eq. (7), we plot  $Y' \equiv C L^{-\alpha} V^{\theta_L}$  vs  $X' \equiv t L^{-\alpha/\beta} V^{(\theta_t + \theta_L)/\beta}$  for different values of  $\theta_t$  and  $\theta_L$ . The best data collapse is found with  $\theta_t = 0.37$  and  $\theta_L = 0.48$ . Using these exponents we form the scaling plot for measurements at five different values of  $H$  and times spanning three decades. From the data collapse in Fig. 4, we conclude that our measurements are fully consistent with our scaling ansatz.

In fact there is some theoretical base for the EDS hypothesis: Kertész and Wolf [17] pointed out that a new diverging length  $\xi \sim |\varepsilon|^{-\nu}$  in the dynamics modifies the scaling of the interface and  $\xi$  must appear in the scaling form  $w(\varepsilon, L, t) \sim \xi^\alpha \mathcal{H}(t', L')$ , where  $L' \equiv L/\xi$ ,  $t' \equiv t/\xi^{z'}$ , and  $z' \equiv \alpha'/\beta'$ . Far from the transition point  $\mathcal{H}(t', L') \sim L'^\alpha \mathcal{F}(t'/L'^{\alpha/\beta})$ , which involves  $w(\varepsilon \neq 0, L, t) \sim \xi^{\alpha' - \alpha} L^\alpha \mathcal{F}(t/L^z \xi^{z - z'})$ . This expression resembles Eq. (7), and the similarity is more than merely formal. Movement of the meniscus consists of pinning and depinning processes [18]. Computer simulations demonstrate [7] that as the driving force  $\varepsilon$  decreases, the surface slows down according to  $V \sim \varepsilon^\theta$  and the linear size of the pinned regimes  $\xi$  diverges  $\xi \sim \varepsilon^{-\nu}$ . These two relations can be integrated, with  $\xi \sim V^{-\nu/\theta}$ . According to this picture, we also expect a new diverging length in our system. The relation  $\bar{h} \sim V^{-1/\Omega}$  points in this direction, although it is clear that Eq. (4) must break down at

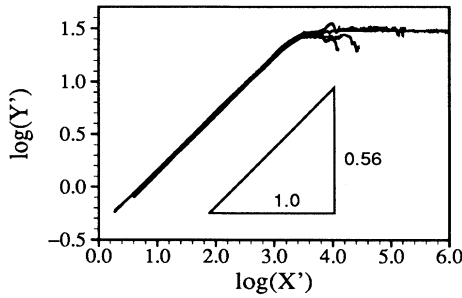


FIG. 4. Scaling plot for five different data sets. In addition to the speeds of sets in Fig. 2, two additional sets are also drawn for  $V = 2.50 \times 10^{-3}$  cm/sec and  $V = 4.20 \times 10^{-3}$  cm/sec;  $Y'$  and  $X'$  are defined in the text. The best result is achieved with exponents  $\beta = 0.56$ ,  $\theta_t = 0.37$ ,  $\theta_L = 0.48$ . According to the scaling function  $\mathcal{F}$  the different data sets collapse on two straight lines, with slopes  $\beta = 0.56$  and zero for early and late times, respectively. The base of the logarithm is 10.

the pinning transition, where  $V = 0$ . If we now replace  $\xi$  by  $V^{-\nu/\theta}$  in  $w(\varepsilon \neq 0, L, t)$ , and compare the result to Eq. (7), we see that there is a mapping between the two relations with  $\alpha' = \alpha + \theta\theta_L/\nu$  and  $z' = z + \theta(\theta_t + \theta_L)/(\beta\nu)$ . Kertész and Wolf demonstrated [17] that  $\alpha'$  and  $z'$  are the characteristic exponents at the transition point between two different morphological phases. It remains an interesting open question whether these exponents have

the same significance at the pinning transition too, and this question requires more experimental investigation.

To summarize, we have studied the temporal behavior of roughening interfaces during vertical imbibition in porous media. The height-height autocorrelation function  $C(t)_{L,V}$  of the meniscus exhibits temporal scaling without crossover. The corresponding exponent is independent of driving force,  $\beta = 0.56 \pm 0.03$ . We conclude that nonlinearity plays an important role in the dynamics of our system. For a compact description of our measurements, we suggest an extended dynamic scaling hypothesis, which describes the characteristic role of the driving force in the presence of quenched disorder, and is fully compatible with the dynamic scaling developed for systems with annealed randomness. From the resulting data collapse, we find  $\theta_t = 0.37$ ,  $\theta_L = 0.48$ . Finally, we note that Rubio *et al.* [19] measured the interface width  $\sigma(l, t)$  versus  $l$  in a different experiment, and they reported a velocity dependent scaling  $w(l) \sim l^{\alpha\nu-0.47}$ , a result consistent with our value of  $\theta_L$ . Although our result suggests that  $\beta$  is independent of the dynamics of the system, it remains to be seen whether the moments of the quenched noise play an important role in determining the universality of exponents.

We would like to thank to the research group of Professor Rama Bansil at Boston University for their kind hospitality. We benefited from discussions with A.-L. Barabási, S. V. Buldyrev, and S. Havlin, and are grateful to J. Kertész and T. Vicsek for helpful comments on the manuscript. This research was supported by OTKA 4167 and by U.S.-Hungarian Joint Fund No. 352.

- [1] See, e.g., T. Vicsek, *Fractal Growth Phenomena*, 2nd ed., Part IV (World Scientific, Singapore, 1992); J. Kertész and T. Vicsek, in *Fractals in Science*, edited by A. Bunde and S. Havlin (Springer-Verlag, Heidelberg, 1994); P. Meakin, *Phys. Rep.* **235**, 189 (1993); T. Halpin-Healey and Y.-C. Zhang, *ibid.* **254**, 215 (1995); A.-L. Barabási and H.E. Stanley, *Fractal Concepts in Surface Growth* (Cambridge University Press, Cambridge, 1995).
- [2] F. Family and T. Vicsek, *J. Phys. A* **18**, L75 (1985).
- [3] S.F. Edwards and D.R. Wilkinson, *Proc. R. Soc. London, Ser. A* **381**, 17 (1982).
- [4] M. Kardar, G. Parisi, and Y.-C. Zhang, *Phys. Rev. Lett.* **56**, 889 (1986).
- [5] R. Bruinsma and G. Aeppli, *Phys. Rev. Lett.* **52**, 1547 (1984); J. Koplik and H. Levine, *Phys. Rev. B* **32**, 280 (1985).
- [6] D.A. Kessler, H. Levine, and Y. Tu, *Phys. Rev. A* **43**, R4551 (1991); S. He, G.L.M.K.S. Kahanda, and P. Wong, *Phys. Rev. Lett.* **69**, 3731 (1992); T. Nattermann *et al.*, *J. Phys. France II* **2**, 1483 (1992).
- [7] L.-H. Tang and H. Leschhorn, *Phys. Rev. A* **45**, R8309 (1992); S.V. Buldyrev, A.-L. Barabási, F. Caserta, S. Havlin, and H.E. Stanley, *ibid.* **45**, R8313 (1992); L.A.N. Amaral, A.-L. Barabási, S.V. Buldyrev, S.T. Harrington, S. Havlin, R. Sadr, and H.E. Stanley, *Phys. Rev. E* **51**, 4655 (1995).
- [8] G. Parisi, *Europhys. Lett.* **17**, 673 (1992).
- [9] Z. Csahók, K. Honda, and T. Vicsek, *J. Phys. A* **26**, L171 (1993); Z. Csahók, K. Honda, E. Somfai, M. Vicsek, and T. Vicsek, *Physica A* **200**, 136 (1993).
- [10] C.S. Nole, B. Koiller, N. Martys, and M. O. Robbins, *Phys. Rev. Lett.* **71**, 2074 (1993).
- [11] See, e.g., M. Matsushita *et al.*, *Phys. Rev. A* **32**, 3814 (1985).
- [12] J.M. Kim, J.M. Kosterlitz, and T. Ala-Nissila, *J. Phys. A* **24**, 1 (1991).
- [13] J. Kertész and D. Wolf, *J. Phys. A* **21**, 747 (1988).
- [14] J.M. López, M.A. Rodríguez, A. Hernández-Machado, and A. Díaz-Guilera (unpublished).
- [15] L.A.N. Amaral, A.-L. Barabási, and H.E. Stanley, *Phys. Rev. Lett.* **73**, 62 (1994).
- [16] L.H. Tang, M. Kardar, and D. Dhar, *Phys. Rev. Lett.* **74**, 920 (1995).
- [17] J. Kertész and D. Wolf, *Phys. Rev. Lett.* **62**, 2571 (1989).
- [18] Z. Olami, I. Procaccia, and R. Zeitak, *Phys. Rev. E* **49**, 1232 (1994).
- [19] M.A. Rubio, C.A. Edwards, A. Dougherty, and J. P. Golub, *Phys. Rev. Lett.* **63**, 1685 (1989).